Heliyon 10 (2024) e23617

Contents lists available at ScienceDirect

Heliyon

journal homepage: www.cell.com/heliyon

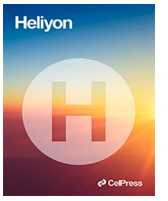

Mechanism of action of *Shaoyao-Gancao* decoction in relieving chronic inflammatory pain via Sema3G protein regulation in the dorsal root ganglion

Rong Lin [a,1], Jun-Gang Gu [a,1], Zhi-Fu Wang [b], Xiao-Xia Zeng [a], Hong-Wei Xiao [a], Jin-Cheng Chen [b], Jian He [c,d,*]

[a] *College of Rehabilitation Medicine, Fujian University of Traditional Chinese Medicine, Fuzhou, 350122, China*
[b] *Affiliated Rehabilitation Hospital, Fujian University of Traditional Chinese Medicine, Fuzhou, 350003, China*
[c] *Fujian University of Traditional Chinese Medicine, Fuzhou, 350122, China*
[d] *Zhangzhou Health Vocational College, Zhangzhou, 363000, China*

A R T I C L E I N F O

Keywords:
CCL2
Chronic inflammatory pain
Dorsal root ganglion
sema3G
IL-6
Shaoyao-Gancao decoction

A B S T R A C T

Objective: The purpose of this study was to analyze the impact of *Shaoyao-Gancao* decoction (SGD) on proteins with significant changes in the dorsal root ganglion (DRG) in rats and to explore the role of the Semaphorin 3G (Sema3G) protein in the DRG and its downstream factors, interleukin-6 (IL-6) and CC-motif chemokine ligand 2(CCL2), in the treatment of chronic inflammatory pain (CIP).

Methods: We created a CIP rat model using 100 μL of complete Freund's adjuvant (CFA) that was injected into the left posterior plantar of rats. Then, we administered SGD intragastrically. We tested the animals for behavioral changes and protein expression levels in DRG pre- and post-drug intervention.

Results: Rats in the SGD group showed significantly increased paw withdrawal threshold (PWT), paw withdrawal latency (PWL), and relative expression levels of the Sema3G protein in the DRG (all $P < 0.05$), while the relative mRNA expression levels of IL-6 and CCL2 in the DRG of the rats were significantly decreased ($P < 0.05$) when compared with the model group.

Conclusion: In this study, we found that *Shaoyao-Gancao* decoction was effective in improving the PWT and PWL of rats with CIP. It reduced CIP by upregulating the expression of Sema3G in the DRG and inhibiting the relative mRNA expression levels of IL-6 and CCL2.

1. Introduction

Chronic inflammatory pain (CIP) refers to the pathological pain caused by the increased excitability of nociceptors in response to the release of pain-causing chemicals. This can change the physiological environment of injured tissue when inflammation occurs in the body. The condition manifests mainly as hyperalgesia and allodynia. *Shaoyao-Gancao* Decoction (SGD) is a traditional Chinese medicine preparation used mainly in the treatment of abdominal pain and acute spasms of the legs and feet, and it was first

* Corresponding author. Fujian University of Traditional Chinese Medicine, No.1 Qiuyang Road, Shangjie Town, Minhou County, Fuzhou City, Fujian, 350122, China.
E-mail address: hejian@fjtcm.edu.cn (J. He).
[1] These authors contributed equally to this study.

https://doi.org/10.1016/j.heliyon.2023.e23617
Received 6 January 2023; Received in revised form 22 November 2023; Accepted 7 December 2023
Available online 12 December 2023

documented in the *Treatise on Febrile Diseases.* [1] Pain disorders and musculoskeletal/joint diseases are treated with SGD due to its strong analgesic effect [2]. It is one of the most commonly used oral analgesics in East Asia [3].

Modern pharmacological studies have confirmed that SGD has anti-spasmodic, analgesic, anti-inflammatory, and anti-allergenic properties and is used in a variety of treatments for cough and asthma relief, neuromuscular blocking, and improving immune regulation [4]. Experimental studies on the anti-inflammatory and analgesic mechanisms of SGD demonstrated that it could relieve the pain symptoms of cervical spondylosis in animal models and reduce the expression levels of the inflammatory factors interleukin-1β (IL-1β), interleukin-6 (IL-6), and tumor necrosis factor-alpha (TNF-α) [5,6]. Additionally, SGD was found to be effective in inhibiting the synthesis and release of microglial inflammasomes in the spinal cord anterior horn, thereby reducing the expression of inflammatory factors [7]. SGD has been shown to intervene in CIP, although the mechanism by which it does so in the dorsal root ganglion (DRG) is not well understood.

The DRG is the gathering point for first-order neurons involved in afferent sensation. It receives and integrates sensory information from the peripheral nerve endings and transmits it to the spinal dorsal horn. Chronic inflammatory pain affects DRG functions, resulting in changes such as protein degradation and abnormal cytokine release [8–10].

In this study, we used whole-protein four-dimensional (4D) label-free quantitative proteomics to detect proteins with significant changes in the DRG as a result of treating CIP with SGD. We followed this with a validation analysis of the differential proteins to offer insights into the analgesic mechanism of SGD. We found that 1,4-alpha-glucan branching enzyme 1 (Gbe1), Myosin regulatory light chain 2 (Myl2), and Semaphorin 3G (Sema3G) were the common differentially expressed proteins. Gbe1 and Myl2 have not been reported previously to be associated with pain or inflammation, whereas Sema3G has been shown to be associated with sleep deprivation and remifentanil-induced hyperalgesia [11], with demonstrated inhibitory effects on inflammatory factors and chemokines in lipopolysaccharide (LPS)-induced inflammation models in vitro [12]. Therefore, for the present study, we selected Sema3G to investigate whether SGD could play an anti-inflammatory and analgesic role in CIP via the regulation of Sema3G.

Abnormal cytokine release in the DRG is thought to cause chronic inflammatory pain. The deficiency of Sema3G in glomerular podocytes has been shown in a previous study [13] to enhance the expression of inflammatory cytokines, including IL-6 and CC-motif chemokine ligand 2(CCL2). Studies in animal models of CIP found that local inflammation and pain induced the upregulation of IL-6 and CCL2 in the DRG [9,14,15]. Therefore, in the current study, we selected IL-6 and CCL2 in the DRG as downstream cytokines.

We can summarize the key theoretical foundations of this study as follows: (1) The occurrence and progression of CIP are closely associated with protein changes in the DRG. (2) SGD has a clear analgesic effect, but its mechanism of inflammation regulation in the DRG requires further investigation.

Based on the above theoretical basis, we hypothesized that SGD is likely to improve CIP by regulating the expression levels of Sema3G, IL-6, and CCL2 in the DRG.

2. Materials and methods

2.1. Animals

We purchased a total of 36 specific-pathogen-free (SPF) male Sprague-Dawley (SD) rats, aged 6–8 weeks and weighing 200 ± 20 g, from the Shanghai SLAC Animal Liability Co., Ltd. (License No. SCXK [Shanghai] 2012–0001). These were raised in the laboratory animal research center at the Fujian University of Traditional Chinese Medicine (License No. SYXK [Fujian] 2020–0002). The feeding environment was maintained at an appropriate temperature and humidity with a 12-h alternating light and dark cycle. The experimental procedure was conducted in strict accordance with the regulations for the use of experimental animals in China and the animal management system of our institution.

The rats were fed a breeding diet for lab rats and mice (manufactured by Beijing HFK Bioscience Co., Ltd., license No. SCXK [Beijing] 2019–0008). The nutritional components of this feed (calculated per kilogram of feed) are shown in Table 1. The animals did not receive any additional food supplements.

Table 1
Nutritional components of the breeding diet (Calculated per kilogram of feed).

Nutritional composition	Content
Crude protein	≥200 g
Crude fat	≥40 g
Moisture	≤100 g
Coarse gray powder	≤80 g
Coarse fiber	≤100 g
Calcium	10–18 g
Phosphorus	6–12 g
Lysine acid	≥13.2 g
Methionine + Cystine	≥7.8 g
Vitamin E	≥120IU

2.2. Drugs and reagents

We used the following drugs and reagents: a bicinchoninic acid (BCA) protein concentration assay kit and a sodium dodecyl sulphate-polyacrylamide gel electrophoresis preparation kit (Wuhan Boster Biological Technology Co., Ltd., China); protein markers, Western antibody diluent, and a hyper-sensitivity electrochemiluminescence kit (Shanghai Beyotime Biotechnology Co., Ltd., China); polyvinylidene fluoride (PVDF) membrane (Millipore, USA); Sema3G primary antibody (Abcam, UK); glyceraldehyde-3-phosphate dehydrogenase (GAPDH) antibody and goat anti-rabbit secondary antibody (Proteintech, USA); GelstainRedTM nucleic acid dye (Suzhou UElandy Biotechnology Co., Ltd., China); DNA extraction reagent and a total RNA extraction kit (Beijing Solarbio Science & Technology Co., Ltd., China); and Sema3G recombinant adenovirus and blank control recombinant adenovirus (Shenzhen Brain Case Biotechnology Co., Ltd., China).

2.3. Instruments

The following instruments were used in this study: a von Frey Pain Threshold Detector (North Medical, USA), a thermal radiation dolorimeter (Chengdu Techman Software Co., Ltd., China), an automatic microplate reader (BioTek, USA), a high-speed refrigerated centrifuge (Eppendorf, Germany), a thermostatic water bath (Tanon Science & Technology Co., Ltd., Shanghai, China), an electrophoresis apparatus, a chemiluminescence imaging system (Bio-Rad, USA), pipettes (Eppendorf, Germany), a water purifier (Thermo Fisher Scientific, USA), a Milli-Q ultra-purified water system (Millipore, USA), a DNA amplification instrument (model 9600) (PE Company, USA), a timsTOF Pro mass spectrometer (Bruker) and a nanoElute ultra-performance liquid chromatography (UPLC) system (Bruker).

3. Methods

3.1. Groups

The research study consisted of the following two experiments:

Experiment 1. We randomly numbered a total of 18 SPF male SD rats and divided them into the following three groups using a random number table: the control group (n = 6), the model group (n = 6), and the SGD group (n = 6). The rats in the control group were injected with 100 μL of normal saline at the left posterior plantar during modeling, while the rats in the model and SGD groups were injected with 100 μL of complete Freund's adjuvant (CFA) at the left posterior plantar.

Experiment 2. We randomly numbered another set of 18 SPF male SD rats, and using a random number table, we divided them into three groups: the control group (n = 6), the model + negative control group (n = 6), and the model + virus overexpression group (n = 6). The rats in the control group were fed normally before modeling and did not receive any intrathecal injections. Four weeks before modeling, the rats in the model + negative control group were injected intrathecally with a blank control recombinant adenovirus (rAAV-hSyn-EGFP), while the rats in the model + virus overexpression group received intrathecal injections of the rAAV-hSyn-Sema3g-P2A-EGFP virus. During modeling, rats in the control group were injected with 100 μL of normal saline at the left posterior plantar, while the rats in the model + negative control group and the model + virus overexpression group were injected with 100 μL of CFA at the left posterior plantar.

3.2. Modeling

All the experimental rats were fasted for 12 h before modeling, with free access to water. The rats were anesthetized with an intraperitoneal injection of 30 mg/kg of 3 % pentobarbital sodium by weight. After the rats were fully anesthetized, 100 μL of CFA was slowly injected subcutaneously at the left posterior plantar using a microsyringe. After modeling, the animals were kept at room temperature (25 °C) to awaken. We closely monitored the body temperature, respiration, heartbeat, and other vital signs of the rats throughout the modeling process. After waking, the rats were placed in cages for subsequent observation.

3.3. Administration

In experiment 1, the rats in the SGD group were administered SGD intragastrically 24 h after the completion of modeling. The decoction was prepared as per the original prescription in the *Treatise on Febrile Diseases* [1] (*Paeonia alba radix* [12 g], honey-fried licorice [12 g]), and the dosage for the rats was calculated according to the daily clinically effective dose for 60-kg adults. The following formula was used: daily dose/rat = dose/kg (human body weight) × conversion factor 6.17 × body weight of each rat (the dose of SGD in adults was 0.4 g/kg [body weight]) [16]. The dose for rats with a standard weight of 150 g was calculated as 0.4 g/kg × 6.17 = 2.468 g/kg. Based on the standard, for rats with a body weight of 250 g, the dosage of SGD was calculated to be about 2.068 g/kg.

After determining the dosage, SGD of the corresponding concentration was prepared based on the intragastric volume of the rats. In this experiment, we used granules (purchased from the traditional Chinese medicine pharmacy of Fujian Rehabilitation Hospital). The rats in the model group were given the same dose of normal saline by gavage every day, while the rats in the control group were catched at the same time every day without other intervention measures. The above interventions were implemented once a day for

seven consecutive days.

3.4. Injection of the virus

Experiment 2 involved injecting a virus directly into the intrathecal space. The rats in the model + negative control group were injected intrathecally with a blank control recombinant adenovirus (rAAV-hSyn-EGFP) (AAV/9, virus titer 5.43 E + 12 vg/mL) 28 days before modeling, while the rats in the model + virus overexpression group received intrathecal injections of the Sema3G recombinant adenovirus (rAAV-hSyn-rSema3g-P2A-EGFP) (AAV/9, virus titer 2.89 E+12 vg/ml), as shown in Fig. 1.

The primer sequence was as follows:

679-F1: TGCCTGAGAGCGCAGGTCGACGCCACCATGGCCCGCTGCTCC, 679-R1: AGCAGGCTGAAGTTAGTAGCTGTGGCTTC-TACCTCCCGGG, 679-F2: CCCGGGAGGTAGAAGCCACAGCTACTAACTTCAGCCTGCT, 679-R2: GGTTGATTATCTCGAGAATTCTCAC TTGTACAGCTCGTC.

After anesthesia with isoflurane inhalation, the spinous space between L5-L6 lumbar vertebrae was exposed, and percutaneous lumbar puncture was performed with 25-μl microsamplers. The hind limb flutter or lateral swing of the rat tail indicated a successful puncture (Fig. 2).

3.5. Paw withdrawal threshold test

The rats underwent a paw withdrawal test (PWT) of the left hindlimb before modeling and on days 1, 3, 5, and 7 after modeling. The test was performed between 8:00 a.m. and 12:00 p.m. Constant ambient temperature and humidity levels were maintained (23 ± 2 °C and 50 ± 2 %, respectively). The measurement was done as per the up-down method [17], and licking, lifting, moving, or foot withdrawal actions by the rats during the stimulation were considered positive reactions. After each stimulation, the next stimulation began once the rats had settled down. The mean value obtained from three measurements was recorded as the test result.

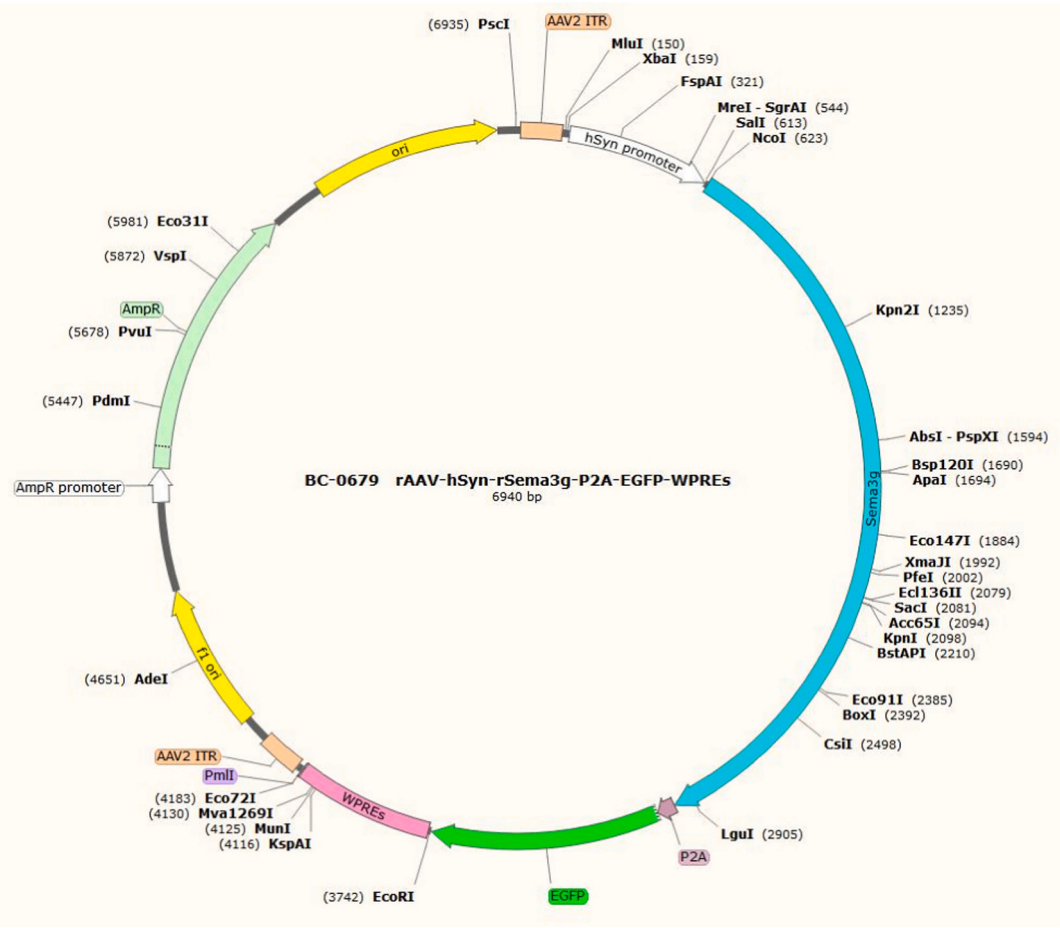

Fig. 1. rAAV-hSyn-rSema3g-P2A-EGFP-WPREs map.

Fig. 2. Successful insertion of the intrathecal catheter.

3.6. Paw withdrawal latency test

We checked the pain response time of the left hindlimb of the rats before modeling and on days 3, 5, and 7 after modeling. The measurement environment was similar to that for the measurement of the PWT. Following the Hargreaves method [18], radiation stopped automatically when the rats began to withdraw their feet, and the time was recorded. The model side foot of each rat was measured three times with an interval of at least 5 min and then averaged.

3.7. Whole-protein 4D label-free quantitative proteomics

(1) We followed the following procedure for protein extraction: The DRG tissues of the rats were collected, weighed, and added to an appropriate amount of lysate. Then they were mixed, sonicated, and left at a low temperature for 30 min. The supernatant was removed, centrifuged, and cryopreserved for later use. We used a BCA kit to determine the protein concentrations.
(2) Trypsin digestion was performed as follows: The same amount of protein was taken from each sample for enzymolysis, and we adjusted the volume for consistency using lysate. Then trichloroacetic acid (TCA) was added to achieve a final concentration of 20 %. Subsequently, the solution was precipitated for 2 h at 4 °C and centrifuged. The supernatant was discarded, and the precipitate was washed two to three times with pre-cooled acetone. After the precipitate dried, tetraethyl ammonium bromide (TEAB) at a final concentration of 200 mM was added. The precipitate was dispersed by sonication, trypsin was added, and enzymolysis was performed overnight. Dithiothreitol was added to achieve a final concentration of 5 mM, and reduction was carried out at 56 °C for 30 min. Then, iodoacetamide was added to achieve a final concentration of 11 mM. The solution was incubated for 15 min at room temperature in a dark place. Finally, the peptide solution was collected to obtain enzymolysis samples.
(3) Liquid chromatography-mass spectrometry was performed as follows: Peptide fragments were dissolved in liquid chromatography mobile phase A and separated using a nanoElute UPLC system. The peptide fragments separated by the UPLC system were injected into a capillary ion source for ionization and analyzed using a timsTOF Pro mass spectrometer.
(4) We performed the following database searches: We retrieved the secondary mass spectrometry data of this experiment using the MaxQuant (V1.6.15.0) software package. The database was RattUS_norvegicus_10116_PR_20201214.FASTA (29,940 sequences), in which a negative database and a common contamination database were added to calculate the false positive rate and eliminate the influence of contaminated proteins on the identification results.
(5) We used the following databases for the bioinformatics analysis: UniPROt-GOA for Gene Ontology (GO) protein annotation, WoLF PSORT for the subcellular localization annotation of differential proteins, and the Kyoto Encyclopedia of Genes and Genomes (KEGG) pathway for annotation, enrichment analysis of protein pathways, and classification of pathways.

3.8. Western blotting

The DRG tissues of the rats were collected, weighed, and added to an appropriate amount of lysate. Then they were mixed, sonicated, and left at a low temperature for 30 min before centrifugation. Next, the supernatant was removed and cryopreserved for later use. We used a BCA kit to determine the protein concentrations. After sample loading at 50 μg/well, gel stacking with 10 % polypropylene gel, electrophoresis at 40 V, separation with separating glue at 100 V, and glue cutting, the target protein and internal reference protein on the corresponding molecular weight band were transferred to a PVDF membrane at 300 mA. The proteins were blocked with 5 % skimmed milk for 2 h, and Sema3G antibody (1:500) and GAPDH antibody (1:5000) were added.

After incubating at 4 °C overnight, the bands were removed and washed with Tris-buffered saline (TBS) + Tween Buffer (TBST)

three times (5 min each time). After the primary antibody reaction, secondary antibodies (Sema3G 1:8000 and GAPDH 1:8000) were added for a 2-h incubation at room temperature. After the secondary antibody reaction, the membrane was washed with TBST three times (5 min each time). An Image-LAB image analysis system was used to mark the gray values of the target and reference proteins, and the expression level of each index was expressed as the comparison value of the gray values of the target protein band and the reference GAPDH band.

3.9. Real-time fluorescent quantitative polymerase chain reaction

The complete DRGs were quickly removed from the anesthetized rats, and the excess liquid on the surface was rinsed with iced normal saline. The ganglia were placed in a centrifuge tube and stored in a liquid nitrogen tank. The DRG tissues were removed from the EP tubes for the measurement of RNA concentrations on Super NANO. We used the miRNA all-in-one TM reverse-transcription quantitative polymerase chain reaction (RT-qPCR) miRNA detection kit for RT reactions and PCR amplification reactions, done under the following reaction conditions: DNA removal: 42 °C for 2 min; RT reaction: 15 min at 50 °C and 2 min at 85 °C. The PCR amplification reaction included pre-degeneration at 95 °C for 5 min, 40 cycles of amplification at 94 °C for 10 s, and annealing and extension at 60 °C for 30 s.

We used a Bio-Rad RT-qPCR instrument for detection and analysis. The primer sequence was as follows: IL-6: GACTTCCAGC-CAGTTGCCTT/CTGGTCTGTTGTGGGTGGTAT; CCL2: GCATCAACCCTAAGGACTTCAG/TTCTCTGTCATACTGGTCACTTCT; and GAPDH: GATGCTGGTGCTGAGTATGRCG/GTGGTGCAGGATGCATTGCTCTGA.

4. Statistical analysis

We used SPSS 23.0 (IBM) statistical software for data analysis. Measurement data of normal distribution were expressed as mean ± standard deviation ($\overline{\chi} \pm s$). The pain behavior data were analyzed using a repeated analysis of variance (ANOVA). If $P > 0.05$ in Mauchly's test of sphericity, we performed a repeated ANOVA. If $P < 0.05$ in Mauchly's test of sphericity, we used a multivariate ANOVA or a degrees-of-freedom correction test.

The statistical analysis of the proteomic analysis of experiment 1 yielded the differentially expressed proteins. In this part of the experiment, we established three sets of biological replicates, and an ANOVA statistical test was performed. Proteins with fold changes >0.001 or <1000 and $P < 0.001$ were defined as significantly differentially expressed proteins. We used a one-way ANOVA for comparisons between multiple groups, the least-significant difference method for pairwise comparisons between groups in cases of homogeneity of variance, and the Games-Howell post-hoc test in cases of heterogeneity of variance. We used a non-parametric test for non-normally distributed data. A P value of <0.05 indicated a statistically significant difference.

5. Results

5.1. Effect of Shaoyao-Gancao decoction on the pain behavior of rats with CIP

The rats were tested for the left lateral plantar PWT before modeling (day 0), one day after modeling (before intervention), and on days 3, 5, and 7 after modeling. We found that the PWT of the rats in all three groups before modeling was above 9 g, and there were no statistically significant differences between the groups ($P > 0.05$). At 1 day post-modeling, the PWT of the rats in the model group and the SGD group was significantly decreased compared with that in the control group ($P < 0.05$). At 3–7 days after the procedure, the PWT of the rats in the model group was significantly decreased compared with that in the blank group ($P < 0.05$), and it remained below 2 g, indicating that the rats were not self-cured and the model was relatively stable. At 7 days post-modeling, the PWT of the rats in the SGD group was significantly increased compared with that in the model group ($P < 0.05$), as shown in Fig. 3.

We tested the rats for left lateral plantar PWL before modeling and on days 3, 5, and 7 after modeling (i.e., after intervention). The

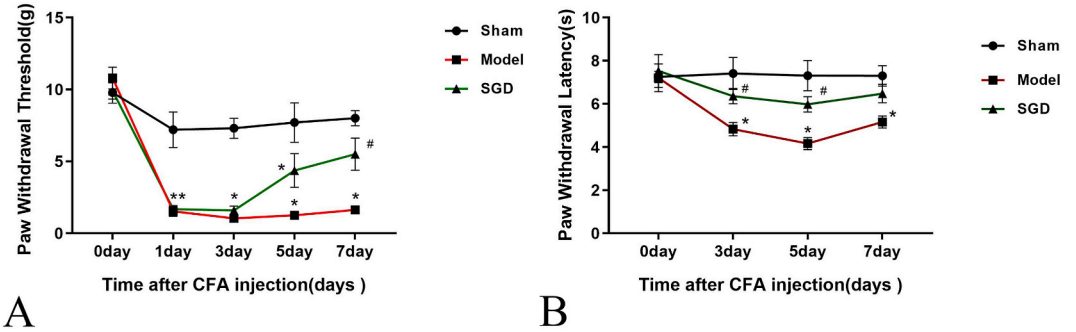

Fig. 3. A. Comparison of the left lateral plantar paw withdrawal threshold of the rats in each group ($\overline{\chi} \pm s$) B. Comparison of the left lateral plantar paw withdrawal latency of the rats in each group ($\overline{\chi} \pm s$)
Note: Compared with the control group, $^{*}P < 0.05$. Note: Compared with the model group, $^{\#} < 0.05$.

PWL of the rats in the three groups before modeling was about 7 s, and the differences between the groups were not statistically significant ($P > 0.05$). After CIP modeling, the PWL of the rats in the model group and the SGD group was significantly decreased ($P < 0.05$). On days 3 and 5 after intervention, the PWL of the rats in the SGD group increased and was significantly higher than that of the rats in the model group ($P < 0.05$), as shown in Fig. 3.

5.2. Effect of Shaoyao-Gancao decoction on the proteomics of DRG in rats with CIP

On day 8 after the operation, we analyzed the total protein expression of the DRG of the rats in each group using whole-protein 4D label-free quantitative proteomics. We found that compared with the control group, the expression levels of a total of 17 proteins were significantly increased in the model group, while in the DRG of the rats in the model group, 52 proteins had significantly decreased expression. Compared with the model group, the expression levels of a total of 465 proteins were significantly decreased, while 243 proteins were significantly increased in the rats of the SGD group, as shown in Fig. 4. With the comparison between the model group and the control group (See Fig. 5A) and the SGD group and the model group (see Fig. 5B), we plotted a differential protein volcano map based on the differential proteins and the protein change degree obtained from the proteomics results.

The GO analysis included biological processes (BP), cellular compartments (CC), and molecular functions (MF). The BP results of this experiment revealed that the differential proteins among the three groups were mainly involved in cellular processes, biological regulation, metabolic processes, and stimulus response. The CC results showed that the differentially expressed proteins were mainly from cells, intracellular proteins, and protein-containing complexes. The MF results revealed that most of the differential proteins exhibited binding activity, catalytic activity, and structural molecular activity, as shown in Fig. 6. Fig. 6A shows the GO annotation entries of the differential proteins in the model group compared with the control group, and Fig. 6B shows the GO annotation entries of the differential proteins in the SGD group compared with the model group.

The subcellular localization annotation of the differential proteins in the model and control groups was mainly in the nucleus and extracellular regions, as shown in Fig. 7A. Compared with the model group, the subcellular localization of differential proteins in the SGD group was mainly in the nucleus and cytoplasm, as shown in Fig. 7B.

The KEGG pathway enrichment analysis showed that, compared with the control group, the upregulated or downregulated proteins in the DRG in the model group were involved mainly in the transforming growth factor-beta (TGF-beta) signaling pathway and the sphingolipid signaling pathway (see Fig. 8A). Compared with the model group, the upregulated or downregulated proteins in the DRG in the SGD group were involved mainly in the adipocytokine signaling pathway (see Fig. 8B), the metabolism of xenobiotics by cytochrome P450, chemical carcinogenesis, porphyrin and chlorophyll metabolism, Th1 and Th2 cell differentiation, drug metabolism by cytochrome P450, and other related pathways, as shown in Fig. 9.

5.3. Effect of Shaoyao-Gancao decoction on the relative expression level of Sema3G in the DRG of rats with CIP

To further verify the differential protein Sema3G in the proteomics results, we conducted a quantitative analysis using Western blotting. The results showed that in comparison with the control group, the relative protein expression level of Sema3G in the DRG of the rats in the model group decreased ($P < 0.05$), while in comparison with the model group, the relative protein expression level of Sema3G in the DRG of the rats in the SGD group increased ($P < 0.05$), as shown in Figs. 10 and 11, respectively.

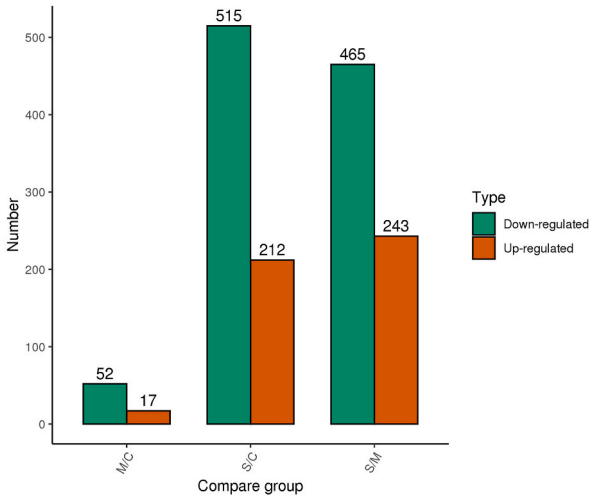

Fig. 4. Number of differential proteins in the dorsal root ganglion of the rats in each group. Note: Red indicates the number of proteins with upregulated expression, and green indicates the number of proteins with downregulated expression.

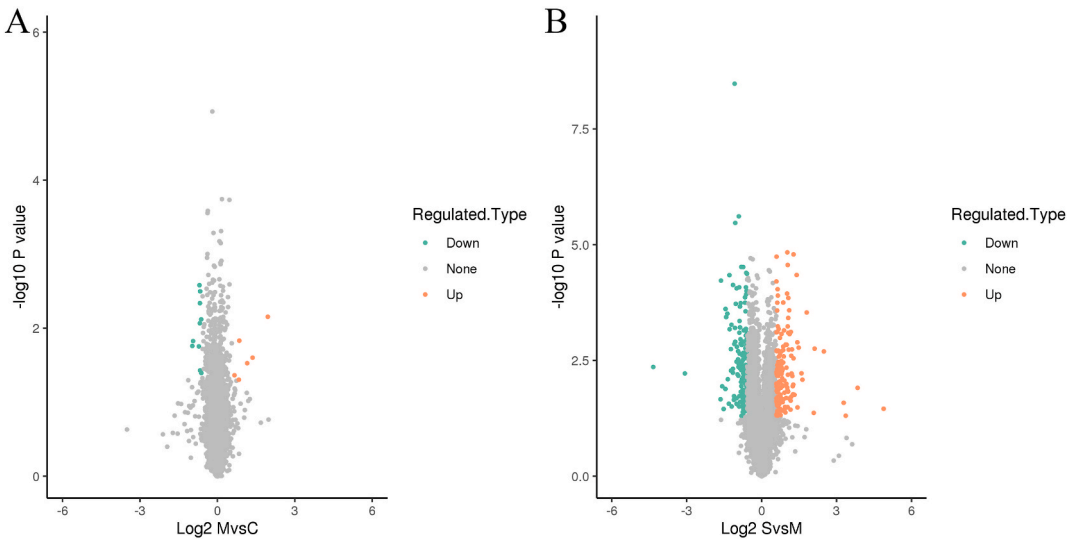

Fig. 5. Volcano plot of differential proteins. Note: The X axis represents the value of protein change degree after Log2 conversion, and the Y axis represents the *P* value of a *t*-test of significant difference after Log10 conversion. The red dot represents a protein with upregulated expression, and the blue dot represents a protein with significantly downregulated expression. A: Model group vs. control group (number of proteins) B: *Shaoyao-Gancao* decoction group vs. model group (number of proteins).

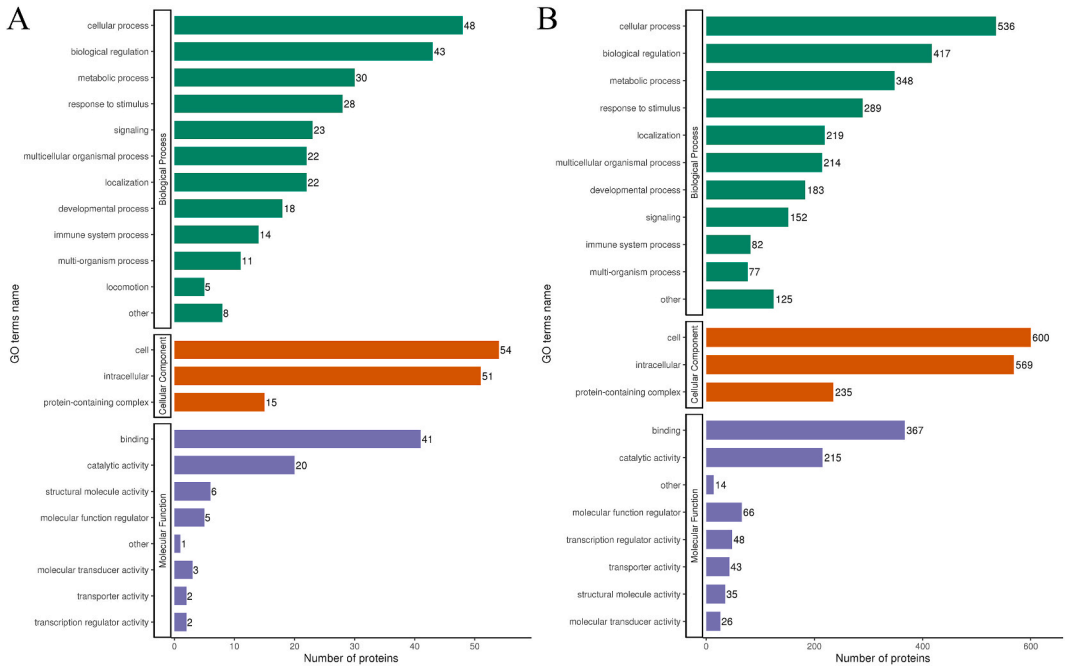

Fig. 6. Gene Ontology (GO) protein annotation. Note: Fig. 6A shows the GO annotation entries of the differential proteins in the model group compared with the control group. Fig. 6B shows the GO annotation entries of the differential proteins in the SGD group compared with the model group. A: Model group vs. blank group B: *Shaoyao-Gancao* decoction group vs. model group.

5.4. Effect of Shaoyao-Gancao decoction on the relative mRNA expression levels of IL-6 and CCL2 in the DRG of rats with CIP

We reviewed the literature to further explore the anti-inflammatory and analgesic mechanisms of SGD and found that a Sema3G deficiency could enhance the expression of inflammatory cytokines, including IL-6 and CCL2, in glomerular podocytes. Therefore, we used real-time PCR to detect the mRNA expression levels of IL-6 and CCL2 in the DRG.

The results showed that in the model group, the relative mRNA expression level of IL-6 in the DRG of the rats was significantly

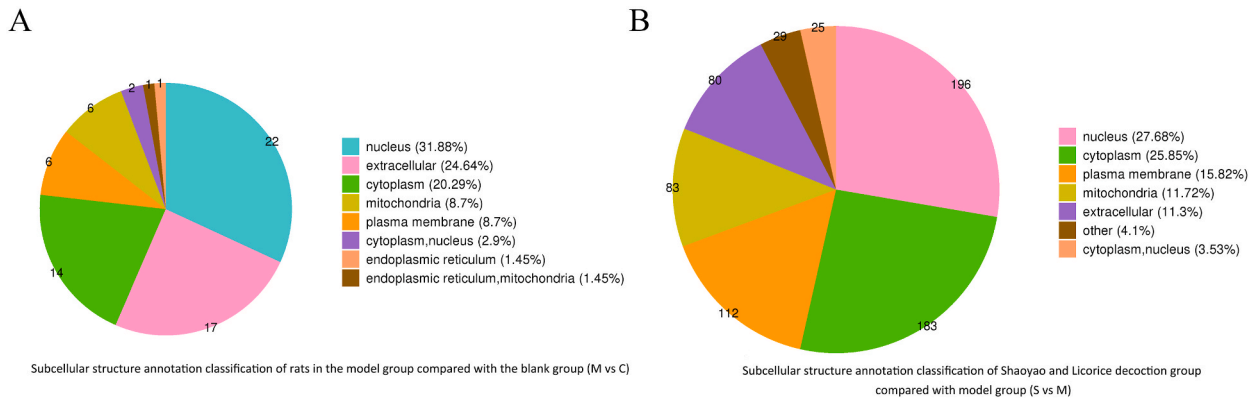

Fig. 7. Subcellular localization annotation. Note: Fig. 7A shows the subcellular localization annotation of differential proteins in the model group compared with the control group. Fig. 7B shows the subcellular localization annotation of different proteins in the SGD group compared with the model group.

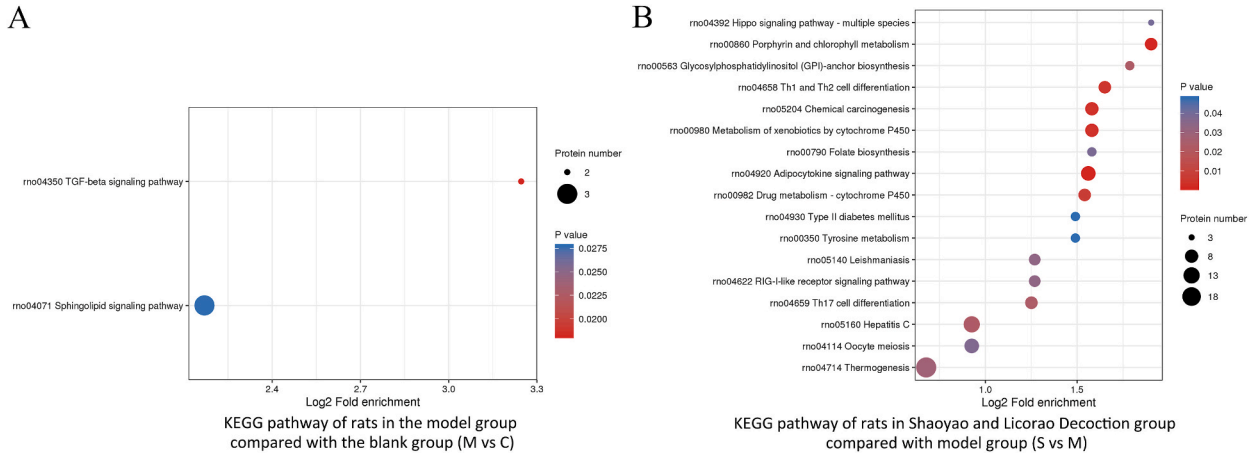

Fig. 8. Bubble diagram of functional enrichment analysis of differential proteins. Note: Fig. 8A shows the functional enrichment distribution of differential proteins in the model group compared with the control group. Fig. 8B shows the functional enrichment distribution of differential proteins in the SGD group compared with the model group.

increased ($P < 0.05$) when compared with the blank group. In the SGD group, the relative mRNA expression level of IL-6 in the DRG of the rats was significantly decreased ($P < 0.05$) when compared with the model group, as shown in Fig. 12A.

In the model group, when compared with the control group, the relative mRNA expression level of CCL2 in the DRG of the rats was significantly increased ($P < 0.05$). Finally, compared with the model group, the relative mRNA expression level of CCL2 in the DRG of the rats in the SGD group was significantly decreased ($P < 0.05$), as shown in Fig. 12B.

5.5. *Effect of intrathecal injection of Sema3G overexpressing virus on the pain behavior of rats with CIP*

We treated rats with intrathecal injections of a recombinant adenovirus overexpressing Sema3G (rAAV-hSyn-rSema3g-P2A-EGFP) or a blank control recombinant adenovirus (rAAV-hSyn-EGFP) to further determine whether the upregulation of Sema3G in the DRG could improve the PWT and PWL after CIP was induced. We tested the rats in each group for the left lateral plantar PWT and PWL before modeling (day 0) and at days 1, 3, 5, and 7 after modeling.

Rats in the three groups had a PWT of >9 g before modeling, and the differences between the groups were not statistically significant ($P > 0.05$). On day 1 after modeling, rats in the model + negative control group and the model + virus overexpression group showed significantly decreased PWT when compared with the control group ($P < 0.05$). On day 7 after modeling, the PWT of the rats in the model + virus overexpression group was significantly increased compared with that in the model + negative control group ($P < 0.05$), as shown in Fig. 13A.

In all three groups, the PWL of the rats was >7 s before modeling, and the differences were not statistically significant ($P > 0.05$). After CIP modeling, the PWL of the rats in the model + negative control group and the model + virus overexpression group was significantly decreased ($P < 0.05$). On days 3, 5, and 7 after modeling, the rats in the model + virus overexpression group showed

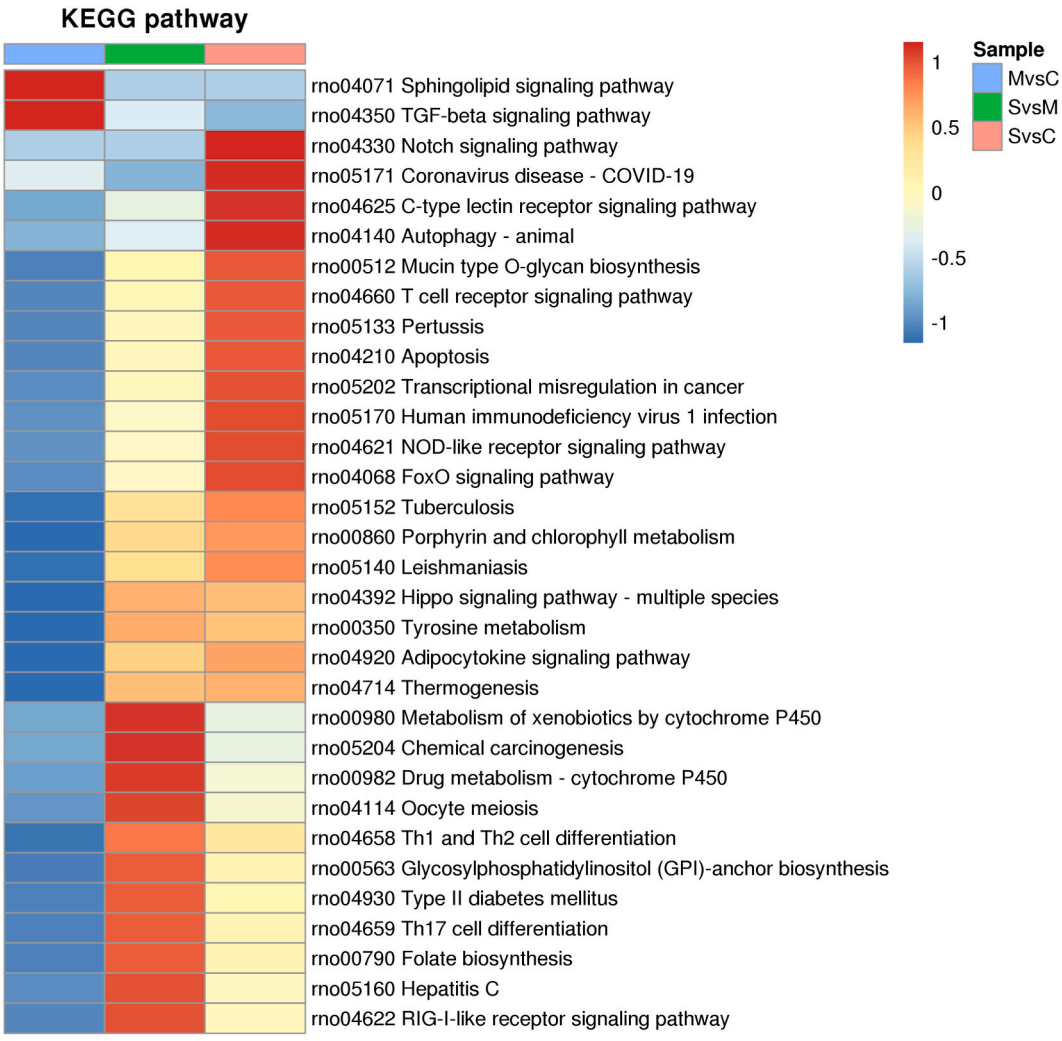

Fig. 9. Cluster analysis heat map of Kyoto Encyclopedia of Genes and Genomes (KEGG) pathway enrichment.

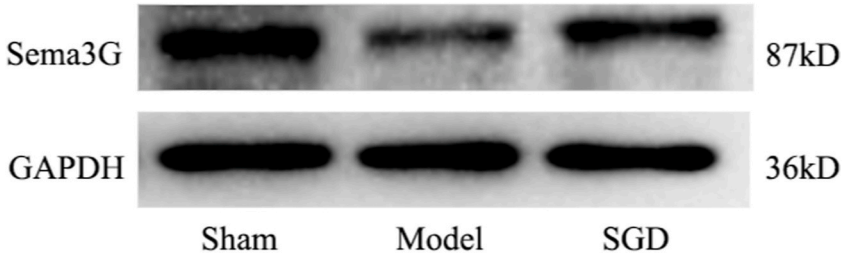

Fig. 10. Relative protein expression of sema3g in the dorsal root ganglion of the rats in each group.

increased PWL, which was significantly higher than in the model + negative control group ($P < 0.05$), as shown in Fig. 13B.

5.6. Effect of intrathecal injection of Sema3G overexpressing virus on the relative mRNA expression levels of IL-6 and CCL2 in the DRG of rats with CIP

To further investigate whether the intrathecal injection of the Sema3G overexpressing virus could inhibit the relative mRNA expression levels of IL-6 and CCL2 in the DRG, we used RT-PCR to detect the relative mRNA expression levels of IL-6 and CCL2 in the DRG on day 7 after modeling (i.e., 35 days after the intrathecal injection of the Sema3G virus).

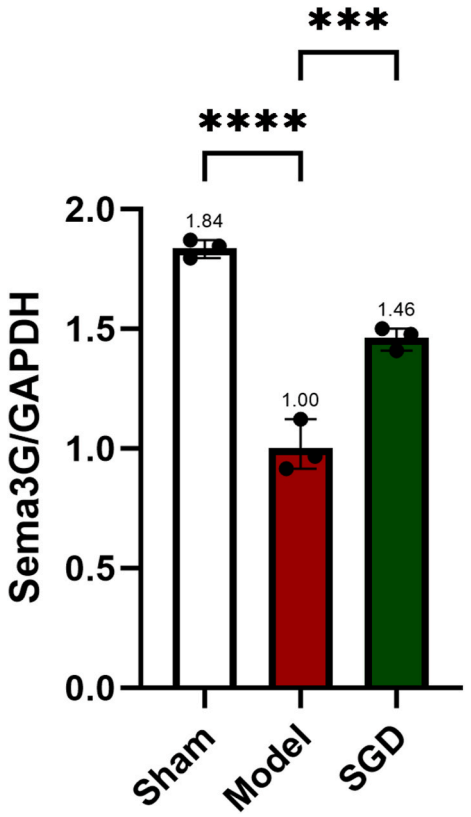

Fig. 11. Comparison of relative protein expression levels of Sema3G in the dorsal root ganglion of the rats in each group ($\overline{\chi} \pm s$). Note: a. Compared with the blank group, $^{****}P < 0.05$. Note: b. Compared with the model group, $^{***}P < 0.05$.

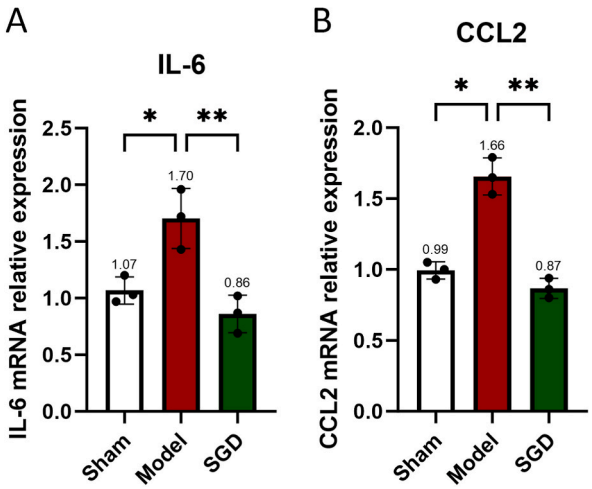

Fig. 12. Comparison of the Relative mRNA Expression Levels of IL-6 and CCL2 in the Dorsal Root Ganglion of the Rats in Each Group. Note: a. Compared with the control group, $^{*}P < 0.05$. Note: b. Compared with the model group, $^{**}P < 0.05$.

The experimental results revealed that the DRG of the rats in the model + negative control group had significantly increased mRNA levels of IL-6 when compared with the control group ($P < 0.05$). In the model + virus overexpression group, compared with the model group, the relative mRNA expression level of IL-6 in the DRG of the rats was significantly decreased ($P < 0.05$), as shown in Fig. 14A.

In comparison with the control group, the relative mRNA expression level of CCL2 in the DRG of the rats in the model + negative control group was significantly increased ($P < 0.05$). Finally, compared with the model group, the relative mRNA expression level of CCL2 in the DRG of the rats in the model + virus overexpression group was significantly decreased ($P < 0.05$), as shown in Fig. 14B.

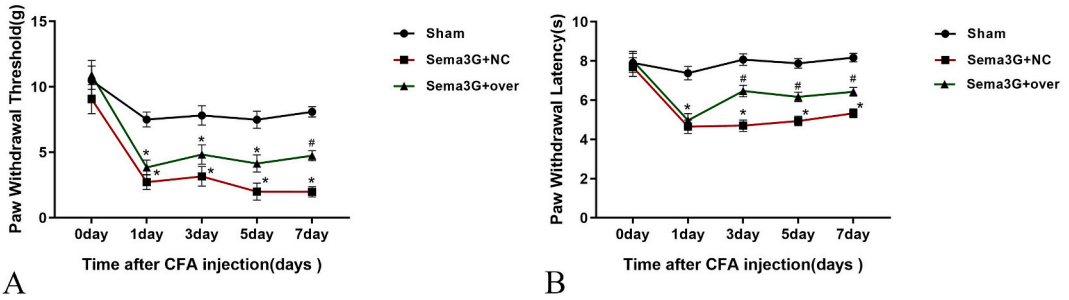

Fig. 13. A. Comparison of left lateral plantar paw withdrawal threshold of the rats in each group ($\overline{\chi} \pm s$) B.Comparison of left lateral plantar paw withdrawal latency of the rats in each group ($\overline{\chi} \pm s$). Note: Compared with the control group, $^{*}P < 0.05$. Note: Compared with the model + negative control group, $^{\#}P < 0.05$.

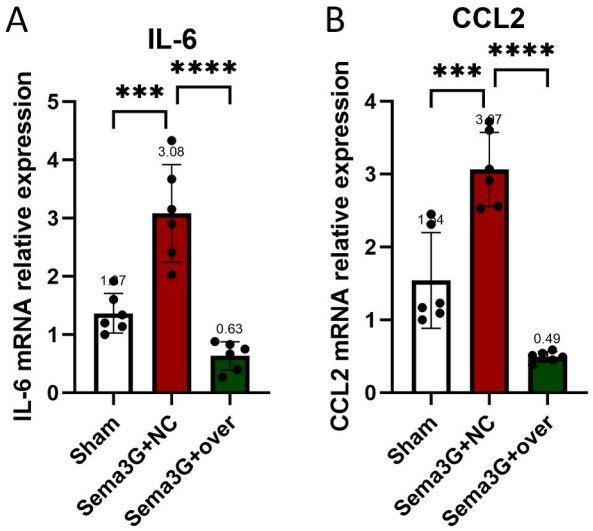

Fig. 14. Comparison of the relative mRNA expression levels of IL-6 and CCL2 in the dorsal root ganglion of the rats in each group. Note: a. Compared with the control group, $^{***}P < 0.05$. Note: b. Compared with the model + negative control group, $^{****}P < 0.05$.

6. Discussion

Shaoyao-Gancao decoction, a standard prescription commonly used in the clinical treatment of pain-related diseases, is one of the most commonly used oral analgesics in East Asia. Hence, understanding its analgesic mechanism assumes much significance.

In this formulation, the ratio of *P. alba* radix and licorice root is closely associated with its anti-inflammatory and analgesic effects. Zhu et al. [19] noted that vinegar-baked *P. alba* radix and honey-fried licorice (1:1) showed the best anti-inflammatory and analgesic effects, while vinegar-baked *P. alba* radix and honey-fried licorice (6:1) had only a weak anti-inflammatory effect and no obvious analgesic efficacy. Based on our earlier clinical research experience and the experimental exploration of the research group, we used *P. alba* radix and honey-fried licorice in a ratio of 1:1 in this experiment.

First described in the *Treatise on Febrile Diseases* [1], SGD is an excellent prescription for relieving spasms and pain [20]. Researchers have used metabolomic analyses to confirm the analgesic effect of paeonol, benzoic acid, paeonol A, paeonolactone C, and other substances in SGD on neuralgia. Liu et al. demonstrated that the active substance in SGD could alleviate trigeminal neuralgia by acting on interleukin-1β, mitogen-activated protein kinase (MAPK) 8, MAPK1, CCL2, and other targets [21]. A study by Zhu et al. found that SGD plays a role in osteoarthritis by regulating cell cycles, apoptosis, drug metabolism, inflammation, and immunity [22].

SGD has shown clear clinical efficacy in the treatment of CIP. In the treatment of lumbar and leg pain associated with lumbar disc herniation, Wu et al. [23] found that SGD + balanced acupuncture was superior to only oral celecoxib capsules; moreover, patients' visual analog scale (VAS) scores and Japanese Orthopedic Association (JOA) scores improved, and the levels of IL-6 and CRP were reduced. In another study on 60 patients with neck pain, SGD showed a good analgesic effect; in the early stage, the pain was significantly relieved after treatment, with a significantly lower VAS score than in a control group [24].

The analgesic effect of SGD has been demonstrated in several basic research studies. For instance, in rats with CFA-induced arthritis, Sui et al. found that it alleviated pain by inhibiting the transient receptor potential vanillin receptor 1 (TRPV1) function in DRG neurons [25]. Yun et al. reported that SGD alleviated visceral hyperalgesia following inflammation by inactivating TRPV1 and

inhibiting the synthesis of 5-hydroxytryptamine [26].

The above studies elucidate, to some extent, the anti-inflammatory and analgesic mechanisms of SGD. In a series of studies on the anti-inflammatory and analgesic effects of SGD, our research group found that SGD could alleviate pain by regulating the expression of miR-146a and miR-155 in the cervical intervertebral disc and neck muscle tissue, thereby inhibiting the downstream inflammatory signaling pathways and reducing the release of TNF-α, IL-1β, IL-6, and other inflammatory factors [6]. Furthermore, in cervical spondylosis model rabbits, SGD could also reduce the local inflammatory response by inhibiting the release of inflammatory factors from the NF-κB signaling pathway [27,28].

The DRG is also sensory ganglion tissue. When stimulus signals from the nerve endings in the limbs are transmitted to neurons in the DRG and the information is integrated in this area, nociceptive sensory neurons project to the dorsal horn of the spinal cord and send signals to secondary neurons, which are projected to the advanced pain center in the hypothalamus and cortex [29].

Numerous studies have found that CIP can lead to changes in the expression of both proteins and cytokines in the DRG. Liu et al. [30,31] found that the Nogo-A protein was significantly increased in the DRG of rats with CIP. The expression levels of CCL2 and its receptor (CCR2) in the DRG were significantly increased in CIP model rats, and CCL2 improved the excitability of nociceptive cells in the DRG. Chen et al. reported that the expression level of p38 MAPK was increased in the DRG of rats with CIP [32]. Niu et al. [33,34] found that CFA injection could upregulate the mRNA expression of IL-6, IL-17, TNF-α, and CCL2 in the ipsilateral DRG. In addition, IL-1β mRNA and COX-2 mRNA and their proteins in the DRG [35] were found to induce the increased expression of CCL2/CCR2, CCL3, CCL21, and endothelial chemokine (C-X-C motif) ligand 1 (CXCL1)/CXCR2.

We used the proteomics technique in the present study to analyze changes in the expression of numerous proteins in the DRG. Rats in the model group showed decreased expression in 52 proteins when compared with the control group, and in the SGD group, there were 212 proteins with increased expression in comparison with the model group. There were three overlapping proteins, for which the encoding genes were *Gbe1*, *Myl2*, and *Sema3G*, respectively. We did not find any relevant reports on the occurrence and development of pain associated with the *Gbe1* and *Myl2* genes in our literature review. One study suggested that inhibiting the expression level of *Sema3G* in the spinal dorsal horn of rats could effectively improve mechanical hyperalgesia and thermal hypersensitivity induced by sleep deprivation and remifentanil and shorten the pain recovery time [36]. However, as there were studies linking *Sema3G* and inflammatory factors, we selected the *Sema3G* gene for verification and analysis in this study.

In the proteomic analysis, the Sema3G protein in the DRG was downregulated in the model group when compared with the control group, while it was upregulated in the SGD group in comparison with the model group. The Western blotting results also confirmed the results of the proteomics analysis, i.e., the relative expression level of the Sema3G protein in the DRG of the rats was downregulated in the model group, while its relative expression level in the rats in the SGD group was upregulated as compared to the model group. Thus, Sema3G expression in the DRG was downregulated during the occurrence and progression of CIP, despite SGD upregulating its expression. Therefore, we can speculate that Sema3G can contribute to the analgesic action of the preparation. This result provides the experimental groundwork for constructing and verifying adenoviruses that overexpress Sema3G.

The Sema3G protein is a member of the Semaphorin family. There is growing evidence that Semaphorin plays an important role in morphological changes and homeostasis across multiple systems, with implications for several biological processes such as cell metastasis and cytokine release [37]. In addition, human genomic analysis has revealed that Semaphorin and its receptors are predisposing or pathogenic genes in schizophrenia, cancer, and degenerative diseases [38,39].

A study [40] revealed that *Sema3A* and *Sema3E* were mainly associated with poor tumor prognosis, while *Sema3G* was generally associated with a tumor survival advantage. The remaining *Sema3* genes showed survival advantages or disadvantages depending on the type of cancer. In addition, all *Sema3* genes were significantly associated with immune infiltration subtypes and correlated with stromal cell infiltration levels and tumor cell stem cells to varying degrees. Other recent studies have shown that *Sema3A* can regulate the degeneration of lumbar intervertebral discs by inhibiting inflammation, antagonizing the activity of vascular endothelial growth factor, and suppressing angiogenesis and the growth and development of vascular endothelial cells [41].

Abnormal vascular hyperplasia is closely associated with the occurrence and development of a variety of diseases. Class-3 Semaphorin family proteins show promise in innovative treatments of diseases via the regulation of blood vessels, nerve ingrowth, and the inflammatory response.

Semaphorin 3G, a new signaling protein in the class-3 Semaphorin family, is a secreted protein of Semaphorin that localizes on chromosome 14 [42]. Exploring the role of the Sema3G protein is a promising direction in disease research [43]. Previous studies have shown that Sema3G supplementation promoted both the formation of healthy vascular networks and the degeneration of diseased vessels during vascular remodeling, suggesting that it has an important protective role in ischemic retinopathy [44,45]. Other studies found that peripheral Sema3G regulates adipocyte differentiation, which is associated with obesity [46]. Gene chip analysis has demonstrated that the expression of Sema3G increases by more than fourfold during adipogenesis. In a pathological state, Sema3G can exert a powerful anti-tumor effect by promoting anti-invasive activity in tumor cells and reducing tumor-associated vascular density.

Semaphorin 3G has also been identified as an important prognostic marker for adult glioma [47]. A recent study found that the Sema3G protein, secreted by cerebrovascular endothelial cells, increases synaptic density and enhances synaptic transmission by acting on Neuropilin-2/PlexinA4 receptors on hippocampal pyramidal neurons. Cerebral vascular endothelium-derived Sema3G knockdown leads to cognitive decline [48]. Furthermore, the Sema3G lentiviral vector can effectively overexpress endogenous Sema3G proteins in human pancreatic cancer cells, thereby inhibiting cell proliferation, invasion, and migration [49]. In an analysis of the in vivo and in vitro functions of Sema3G in the kidney [13], the Sema3G protein, secreted by glomerular podocytes, was found to protect podocytes from inflammatory kidney disease and diabetic nephropathy. The deficiency of Sema3G in podocytes increases the release of inflammatory cytokines and chemokines such as IL-6 and CCL2.

In summary, Sema3G has an anti-inflammatory function as it can inhibit the expression of inflammatory factors and chemokines in

glomerular podocytes. Research on the Sema3G protein has benefited many disorders such as retinopathy, obesity, glioma, cognitive dysfunction, and diabetic nephropathy [13,44–47].

In the present study, after the plantar injection of CFA, we found that the relative mRNA expression levels of IL-6 and CCL2 in the DRG of the rats in the model group were significantly higher than those in the control group. This was consistent with our observations of obvious redness and swelling of the foot on the modeling side and the PWT and PWL values showing a significant downward trend. In the DRG samples obtained from the rats seven days after the administration of SGD, the relative mRNA expression levels of IL-6 and CCL2 were significantly decreased compared with those of the model group. This was consistent with the downward trend in the PWT and PWL values of the rats in the SGD group. These findings indicate that SGD reduced the pain threshold in the rats with CIP by downregulating the relative mRNA expression levels of IL-6 and CCL2 in the DRG, demonstrating the possible analgesic mechanism of the preparation.

Pain and cytokines are closely connected. The most commonly tested biomarker for chronic inflammation is IL-6, which is involved in the initiation and regulation of inflammation [50]. Increased levels of IL-6 can be seen in animal models of neuropathic pain, while decreases in IL-6 levels can inhibit the development of paralgesia. The expression of IL-6 is enhanced in response to environmental stress factors such as infection and tissue damage, and this triggers alarm signals and activates the host's defense mechanisms against stress. Specifically, CCL2 can induce the aggregation of monocytes at the sites of inflammation, traumatic infection, toxin exposure, and ischemia [51].

In addition to its recognized proinflammatory effect, many studies have suggested that CCL2 is associated with pain [52,53] due to its role as a neuron-microglial signaling factor in the development of neuropathic pain. In the case of peripheral chronic inflammation, CCL2 synthesized and released by DRG neurons directly excites nociceptive neurons via autocrine and/or paracrine processes. In a classic CIP model, CFA-induced paw swelling in rats caused an increased expression of CCL2/CCR2 and IL-6 in the ipsilateral DRG. However, treating rats with CFA-induced inflammatory pain with tripterine significantly downregulated the relative mRNA expression levels of IL-6 and CCL2 in the DRG and alleviated pain symptoms [35].

In the present study, our RT-PCR results were consistent with the above findings, indicating that the pain symptoms of rats with CIP were alleviated by the downregulation of the relative mRNA expression levels of IL-6 and CCL2.

To promote complete expression, in the present study, we intrathecally injected adenovirus at L4/5 four weeks before modeling. In experiment 2, the local injection of rAAV-hSyn-rSema3g-P2A-EGFP into the DRG at L4/5 improved the PWT and PWL in the rats with CIP. The PWT in the model + virus overexpression group was significantly increased at 35 days after the injection of the virus when compared with the model + negative control group, and the PWL was significantly increased on days 31, 33, and 35 after injection. This was similar to the efficacy observed in the rats with CIP who were treated with SGD in experiment 1. This indicated that the overexpression of the Sema3G protein with rAAV-hSyn-rSema3g-P2A-EGFP relieved pain, and the optimal treatment effect was seen 31 days after the intrathecal virus injection. Thus, the intrathecal injection of rAAV-hSyn-rSema3g-P2A-EGFP alleviated inflammatory pain symptoms caused by the plantar injection of CFA.

Our results also indicated that the intrathecal injection of the blank control virus did not affect the relative mRNA expression levels of IL-6 and CCL2, i.e., the relative mRNA expression levels of IL-6 and CCL2 in the DRG of the rats in the model + negative control group were significantly higher than those in the control group after CIP modeling. The intrathecal injection of rAAV-hSyn-rSema3g-P2A-EGFP effectively inhibited the relative mRNA expression levels of IL-6 and CCL2 in the DRG. This was similar to a result in the experiment in which the relative mRNA expression levels of IL-6 and CCL2 revealed a consistent downward trend in the DRG of the rats with CIP after the administration of SGD.

Therefore, it is reasonable to speculate that intrathecally injecting rAAV-hSyn-rSema3g-P2A-EGFP might alleviate CIP by inhibiting the relative mRNA expression levels of IL-6 and CCL2. The knockdown of Sema3G expression in the DRG by the rAAV-hSyn-rSema3g-P2A-EGFP virus might play a similar role to that of SGD.

The limitations of the study are as follows: First, we did not explore the specific binding mechanism of Sema3G and its ligand Npn2 in detail. Sema3G and Npn2 are receptor-ligand relationships with high binding affinity. We did not study whether SGD affects the binding processes of Sema3G and Npn2 or the molecular mechanisms underlying this. Besides, due to time and resource limitations in this study, we did not verify the differential proteins Gbe1 and Myl2, but we discussed the correlation between Gbe1 and Myl2 and the occurrence and development of chronic inflammatory pain. In order to obtain insights into the analgesic mechanism of SGD, the influence of Gbe1 and Myl2 on chronic inflammatory pain needs to be further considered. As a newly discovered protein, Sema3G has broad prospects in disease research. The current exploration of Sema3G is mainly in the field of oncology and cancer. In order to give play to the greater reference value of basic research in clinical practice, the possible regulatory mechanism of Sema3G in the treatment of cancer pain by SGD needs to be subsequently considered.

In conclusion, in this study, we found that SGD improved the PWT and PWL in rats with CIP. The decoction improved CIP by upregulating the expression of Sema3G in the DRG and inhibiting the relative mRNA expression levels of both IL-6 and CCL2.

Ethics approval and consent to participate

This study was conducted with approval from the Ethics Committee of Fujian University of Traditional Chinese Medicine. All procedures performed in this study involving human participants were in accordance with ethical standards of institutional and/or national research committee and in compliance with the Declaration of Helsinki. Each enrolled patient signed an informed consent form to use their samples and records for scientific research.

Consent for publication

Not applicable.

Data availability

The data associated with this study has not been deposited into a publicly available repository.
The data will be made available on request.

Funding

This work was supported by the National Key Research and Development Program of China (Grant Nos.: 2022YFC2009700, 2022YFC2009701, 2022YFC2009704).

Authors' contributions

Rong Lin: Analysis and interpretation of data, drafting the article, final approval of the version submitted. Jungang Gu: Acquisition of data, critical revision of the manuscript for intellectual content, final approval of the version submitted. Zhifu Wang: Conception and design of the research, critical revision of the manuscript for intellectual content, final approval of the version submitted. Xiaoxia Zeng: Acquisition of data, critical revision of the manuscript for intellectual content, final approval of the version submitted. Hongwei Xiao: Acquisition of data, critical revision of the manuscript for intellectual content, final approval of the version submitted. Jincheng Chen: Analysis and interpretation of data, critical revision of the manuscript for intellectual content, final approval of the version submitted. Jian He: Conception and design of the research, analysis and interpretation of data, critical revision of the manuscript for intellectual content, final approval of the version submitted.

CRediT authorship contribution statement

Rong Lin: Writing - original draft, Formal analysis. **Jun-Gang Gu:** Writing - review & editing, Data curation. **Zhi-Fu Wang:** Writing - review & editing, Conceptualization. **Xiao-Xia Zeng:** Writing - review & editing, Data curation. **Hong-Wei Xiao:** Writing - review & editing, Data curation. **Jin-Cheng Chen:** Writing - review & editing, Formal analysis. **Jian He:** Writing - review & editing, Funding acquisition, Formal analysis, Conceptualization.

Declaration of competing interest

The authors declare that they have no known competing financial interests or personal relationships that could have appeared to influence the work reported in this paper.

Acknowledgements

We would like to acknowledge the hard and dedicated work of all the staff that implemented the intervention and evaluation components of the study.

Appendix A. Supplementary data

Supplementary data to this article can be found online at https://doi.org/10.1016/j.heliyon.2023.e23617.

References

[1] K. Zhao, N. Shi, Z. Sa, H.X. Wang, C.H. Lu, X.Y. Xu, Text mining and analysis of treatise on febrile diseases based on natural language processing, World J Tradit Chin Med 6 (2020) 67–73.
[2] Y.H. Ning, C.W. Guo, Analysis on the clinical research of Shaoyao gancao decoction according to 21 articles, Guiding Journal of Traditional Chinese Medicine and Pharmacology 23 (3) (2017) 83–84.
[3] T. Ushida, D. Matsui, T. Inoue, et al., Recent prescription status of oral analgesics in Japan in real-world clinical settings: retrospective study using a large-scale prescription database, Expet Opin. Pharmacother. 20 (16) (2019) 2041–2052.
[4] G.W. Zhu, G.J. Zhang, M. Wang, et al., Research situation about origin, active components alignment and phramacological actions of Shaoyao Gancao Decoction, China Journal of Traditional Chinese Medicine and Pharmacy 30 (8) (2015) 2865–2869.
[5] J. He, R. Lin, Y.F. Zhang, et al., Study on the effects and mechanism of Shaoyao Gancao Decoction in reducing cervical intervertebral disc inflammation injury in rabbits by inhibiting NF-κB signaling pathway, China Journal of Traditional Chinese Medicine and Pharmacy 35 (8) (2020) 3885–3889.
[6] J.C. Chen, R. Lin, Y.F. Zhang, et al., Regulation of NF based on miR-146a- κB signal pathway to explore the mechanism of Shaoyao Gancao Decoction in treating inflammation injury of posterior cervical muscles in rabbits with cervical spondylosis, Rehabil. Med. 30 (3) (2020) 206–211.
[7] F.J. Yang, D.W. Wu, J. He, Based on NLRP3 inflammasome, to explore the anti-inflammatory and analgesic mechanism of Shaoyao Gancao Decoction on rats with cervical spondylotic radiculopathy, Fujian Journal of Traditional Chinese Medicine 52 (5) (2021) 53–54.

[8] P. Luo, J. Shao, Y. Jiao, et al., CC chemokine ligand 2 (CCL2) enhances TTX-sensitive sodium channel activity of primary afferent neurons in the complete Freud adjuvant-induced inflammatory pain model, Acta Biochim. Biophys. Sin. 50 (12) (2018) 1219–1226.
[9] T. Zhang, N. Zhang, R. Zhang, et al., Preemptive intrathecal administration of endomorphins relieves inflammatory pain in male mice via inhibition of p38 MAPK signaling and regulation of inflammatory cytokines, J. Neuroinflammation 15 (1) (2018) 320.
[10] D.L. Cao, B. Qian, Z.J. Zhang, et al., Chemokine receptor CXCR2 in dorsal root ganglion contributes to the maintenance of inflammatory pain, Brain Res. Bull. 127 (2016) 219–225.
[11] C.C. Song, The Regulatory Mechanism of Semaphorin 3G on Synaptic Plasticity in Sleep Deprived Remifentanil Hyperalgesia Rats, Tianjin Medical University, 2020.
[12] R. Ishibashi, M. Takemoto, Y. Akimoto, et al., A novel podocyte gene, semaphorin 3G, protects glomerular podocyte from lipopolysaccharide-induced inflammation, Sci. Rep. 6 (2016 May 16), 25955.
[13] R. Ishibashi, M. Takemoto, Y. Akimoto, et al., A novel podocyte gene, semaphorin 3G, protects glomerular podocyte from lipopolysaccharide-induced inflammation, Sci. Rep. 6 (2016), 25955.
[14] X.J. Song, Molecular biological mechanism of peripheral nerve transduction of pain signal, Chin. J. Prev. Med. 22 (1) (2016) 2–7.
[15] X. Wang, W.Z. Li, Research status of mechanism of electroacupuncture in treating inflammatory pain, Journal of Clinical Acupuncture and Moxibustion 32 (2) (2016) 93–95.
[16] Us Food and Drug Administration, Estimating the maximum safe starting dose in initial clinical trials for therapeutics in adult healthy volunteers. Food and Drug Administration, 2005. Retrieved 24 August 2018, from, https://www.fda.gov/media/72309/download.
[17] S.R. Chaplan, F.W. Bach, J.W. Pogrel, et al., Quantitative assessment of tactile allodynia in the rat paw, J. Neurosci. Methods 53 (1) (1994) 55–63.
[18] K. Hargreaves, R. Dubner, F. Brown, et al., A new and sensitive method for measuring thermal nociception in cutaneous hyperalgesia, Pain 32 (1) (1988) 77–88.
[19] G.W. Zhu, G.J. Zhang, M. Wang, Influence of compatibility components combination and proportion on the anti-inflammatory and analgesic effects of peony and licorice decoctions, Pharmaceutical and Clinical Research 22 (4) (2014) 323–325.
[20] L.F. Wu, Y.T. Li, Y.Z. Tang, et al., Research progress on chemical constituents and pharmacological activities of Shaoyao Gancao Decoction, Drug Evaluation Research 44 (6) (2021) 1354–1360.
[21] Y.R. Liu, C.Y. Shi, L. Li, Discussion on the potential mechanism of shaoyao-gancao based on bioinformatics, J. Qingdao Univ. (Nat. Sci. Ed.) 34 (3) (2021) 63–70.
[22] N. Zhu, J. Hou, G. Ma, et al., Network pharmacology identifies the mechanisms of action of Shaoyao gancao decoction in the treatment of osteoarthritis, Med Sci Monit 25 (2019) 6051–6073.
[23] J.L. Wu, H.T. Su, Y.H. Liang, et al., Clinical study on Shaoyao gancao tang combined with balance needle for lumbocrural pain caused by lumbar disc herniation, Journal of New Chinese Medicine 53 (14) (2021) 10–14.
[24] J. He, J.C. Chen, S.J. Chen, Treatment of 60 cases of cervical spondylosis with Shaoyao gancao decoction, Fujian Journal of Traditional Chinese Medicine 45 (1) (2014) 37–38.
[25] F. Sui, H.Y. Zhou, J. Meng, et al., A Chinese herbal decoction, shaoyao-gancao tang, exerts analgesic effect by down-regulating the TRPV1 channel in a rat model of arthritic pain, Am. J. Chin. Med. 44 (7) (2016) 1363–1378.
[26] Y.Y. Shao, Y.T. Guo, J.P. Gao, et al., Shaoyao-Gancao decoction relieves visceral hyperalgesia in TNBS-induced postinflammatory irritable bowel syndrome via inactivating transient receptor potential vanilloid type 1 and reducing serotonin synthesis, Evid Based Complement Alternat Med 2020 (2020), 7830280.
[27] J. He, R. Lin, Y. Zhang, et al., Study on the effects and mechanism of Shaoyao Gancao Decoction in reducing cervical intervertebral disc inflammation injury in rabbits by inhibiting NF-κB signaling pathway, China Journal of Traditional Chinese Medicine and Pharmacy 35 (8) (2020) 3885–3889.
[28] J. Chen, R. Lin, Y. Zhang, et al., Effect of Shaoyao gancao decoction on inflammatory injury of posterior cervical muscle based on miR-146a regulation of NF-κB signaling pathway, Rehabil. Med. 30 (3) (2020) 206–211.
[29] J.Z. Liu, Progress of dorsal root ganglia in mechanism of pain, Chinese Journal of Contemporary Neurology and Neurosurgery 18 (10) (2018) 705–708.
[30] H.C. Liu, Identification of a new functional domain of Nogo-A that promotes inflammatory pain and inhibits neurite growth through binding to NgR1, Chin. J. Prev. Med. 27 (3) (2021) 195.
[31] Q.G. Hu, H.C. Liu, L. Chen, et al., Nogo-A in the rat dorsal root ganglion promotes the polymerization of tubulin and inflammatory heat hyperalgesia, Acta Anat. Sin. 50 (5) (2019) 549–553.
[32] C.S. Chen, X.M. Wan, F. Shi, et al., Expression of P38MAPK and its CCR2 regulation in rat dorsal root ganglion in peripheral inflammatory pain, Chin. J. Prev. Med. 21 (10) (2015) 750–754.
[33] Q. Niu, The Role and Mechanism of Dorsal Root Ganglion Mzf1 in CFA Induced Chronic Inflammatory Pain in Rats, Zhengzhou University, 2020.
[34] Q. Niu, F. Xing, H.W. Gu, et al., Upregulation of myeloid zinc finger 1 in dorsal root ganglion via regulating matrix metalloproteinase-2/9 and voltage-gated potassium 1.2 expression contributes to complete Freund's adjuvant-induced inflammatory pain, Neuroscience 432 (2020) 174–187.
[35] X. Zhang, W. Zhao, X. Liu, et al., Celastrol ameliorates inflammatory pain and modulates HMGB1/NF-κB signaling pathway in dorsal root ganglion, Neurosci. Lett. 692 (2019) 83–89.
[36] C.C. Song, The Regulatory Mechanism of Semaphorin 3G on Synaptic Plasticity in Sleep Deprived Remifentanil Hyperalgesia Rats, Tianjin Medical University, 2020.
[37] L.T. Alto, J.R. Terman, Semaphorins and their signaling mechanisms, Methods Mol. Biol. 1493 (2017) 1–25.
[38] L.H. Chen, E.Y. Cuang, Importance of semaphorins in cancer immunity, Transl. Lung Cancer Res. 8 (Suppl 4) (2019) S468–S470.
[39] F. Mann, S. Chauvet, G. Rougon, Semaphorins in development and adult brain: implication for neurological diseases, Prog. Neurobiol. 82 (2) (2007) 57–79.
[40] X. Zhang, B. Klamer, J. Li, et al., A pan-cancer study of class-3 semaphorins as therapeutic targets in cancer, BMC Med. Genom. 13 (Suppl 5) (2020) 45.
[41] L. Xin, W.X. Xu, J. Wang, et al., Current advances in research of semaphorin 3A:a potential target for the treatment of nospecific low back pain, China J. Orthop. Traumatol. 34 (6) (2021) 589–592.
[42] M. Taniguchi, T. Masuda, M. Fukaya, et al., Identification and characterization of a novel member of murine semaphorin family, Gene Cell. 10 (8) (2005) 785–792.
[43] D. Fard, L. Tamagnone, Semaphorins in health and disease, Cytokine Growth Factor Rev. 57 (2021) 55–63.
[44] D.Y. Chen, N.H. Sun, X. Chen, et al., Endothelium-derived semaphorin 3G attenuates ischemic retinopathy by coordinating β-catenin-dependent vascular remodeling, J. Clin. Invest. 131 (4) (2021).
[45] D. Valdembri, D. Regano, F. Maione, et al., Class 3 semaphorins in cardiovascular development, Cell Adh Migr 10 (6) (2016) 641–651.
[46] M. Liu, S. Xie, W. Liu, et al., Mechanism of SEMA3G knockdown-mediated attenuation of high-fat diet-induced obesity, J. Endocrinol. 244 (1) (2020) 223–236.
[47] L. Karayan-Tapon, M. Wager, J. Guilhot, et al., Semaphorin, neuropilin and VEGF expression in glial tumours: SEMA3G, a prognostic marker? Br. J. Cancer 99 (7) (2008) 1153–1160.
[48] C. Tan, N. Lu, C. Wang, et al., Endothelium-derived semaphorin 3G regulates hippocampal synaptic structure and plasticity via neuropilin-2/PlexinA4, Neuron 101 (5) (2019 Mar 6) 920–937.e13.
[49] Z.F. Gao, X. Gao, Y.N. Wu, et al., Effects of SEMA3G overexpression mediated by lentivirus on human pancreatic cancer cell line PANC-1, Basic & Clin. Med. 36 (7) (2016) 891–895.
[50] S.L. Teng, W. Liu, Y.N. Yu, et al., Research progresses of the relationship between interleukin-6 and pain or painful diseases:a literature review, Chinese Journal Of Painology 17 (2) (2021) 206–211.
[51] Y.J. Gao, Z.J. Zhang, D.L. Cao, Chemokine-Mediated neuroinfl ammation and neuropathic pain, Chinese Journal of Cell Biology 36 (3) (2014) 297–307.
[52] M.A. Dansereau, É. Midavaine, V. Bégin-Lavallée, et al., Mechanistic insights into the role of the chemokine CCL2/CCR2 axis in dorsal root ganglia to peripheral inflammation and pain hypersensitivity, J. Neuroinflammation 18 (1) (2021) 79.
[53] Q. Liu, S.P. Hu, Research progress of the role of chemokines in inflammatory pain, Journal of Qiqihar Medical University 43 (2) (2022) 178–183.